TRANSIENT STABILITY AUGMENTATION BY PROGRAMMED POWER ANGLE RELATIONSHIP USING UNIFIED POWER FLOW CONTROLLER

K R Padiyar and S Krishna

ABSTRACT

Improvement in transient stability can be achieved by adequate system design and discrete supplementary controllers. The emerging Flexible AC Transmission System (FACTS) controllers are considered to be suitable for this purpose due to their speed and flexibility. The Unified Power Flow Controller (UPFC) is a voltage source converter based FACTS controller which injects a series voltage and a shunt current. In this paper, a control strategy is developed to achieve maximal improvement in transient stability using UPFC. It is shown that for a single machine infinite bus system, maximal improvement in transient stability can be achieved by maximizing the electrical power output of the generator w.r.t. the control variables. This result can be extended to multimachine systems and maximizing power flow on a critical line can improve transient stability. The control strategy is evaluated by a simulation study on the 10 generator 39 bus New England system.

INTRODUCTION

There are several discrete supplementary controllers [1,2] which can be initiated following a large disturbance. A comprehensive review of angle stability controls is presented in [3]. Braking resistors and switched series capacitors were among the earliest controllers used to enhance transient stability by changing the network parameters. In recent years, Flexible AC Transmission System (FACTS) controllers are considered to be viable solution to the problem of transient stability, due to their speed and flexibility.

FACTS controllers based on voltage source converters use turn off devices like Gate Turn-Off Thyristors (GTO) [4]. The magnitude and angle of the fundamental frequency voltage injected by the converter is varied by controlling the switching instants of the GTO devices. These type of FACTS controllers have the advantages of reduced equipment size and improved performance compared to variable impedance type controllers. Unified Power Flow Controller (UPFC) is a voltage source converter based FACTS controller which injects a series voltage and a shunt current. The series and shunt branches can generate/absorb reactive power independently and the two branches can exchange real power; therefore UPFC has three degrees of freedom.

UPFC is a versatile controller which can perform the functions of Static Synchronous Compensator (STATCOM) and Static Synchronous Series Compensator (SSSC). Padiyar and Kulkarni [5] propose a control strategy for UPFC to control real power flow through the line, while regulating magnitudes of the voltages at its two ports. Padiyar and Uma Rao [6] present a control scheme for the series injected voltage of the UPFC to damp power oscillations and improve transient stability.

Mihalic et *al* [7] propose maximization of power using UPFC for improvement in transient stability of a single machine infinite bus (SMIB) system. Bian et *al* [8] propose a control strategy to increase power transfer between two large systems during a contingency, using UPFC, while considering the operational constraints.

Padiyar and Uma Rao [9] devised a discrete control strategy for a Thyristor Controlled Series Compensator for transient stability improvement, using the concept of potential energy in a line. They have shown that under certain assumptions it is possible to express the potential energy of a system represented by classical model, as sum of energies in the lines belonging to a cutset. This result is applicable even if the generators are represented by detailed (1.1) model [10]. It is further shown in [10] that the system kinetic energy can be expressed as a function of the rate of change of phase angle across a line belonging to the cutset.

In this paper, a control strategy is derived for UPFC for maximal improvement in transient stability. The control strategy is based on the idea of maximizing energy margin which is a measure of transient stability. The control strategy is derived for a SMIB system. The extension to the multimachine system is based on the energy function given in [10].

CONTROL STRATEGY

The SMIB system with UPFC shown in fig. 1 is used to derive the control strategy. The generator is represented by the classical model. The series and shunt branches of the UPFC are represented by voltage and current sources ($V\angle\phi$ and $I\angle\psi$) respectively.

The transient energy function for the SMIB system is defined as

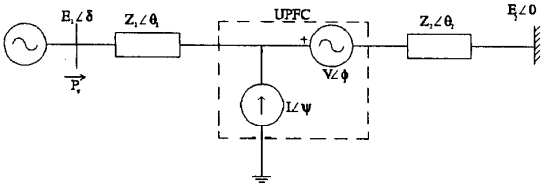

Fig. 1 SMIB system

$$W = W_1 + W_2 \tag{1}$$

W_1 is the kinetic energy and W_2 is the potential energy given by

$$W_1 = \frac{1}{2} M\omega^2 \tag{2}$$

$$W_2 = \int_{\delta_o}^{\delta} (P_e - P_m)\mathrm{d}\delta \tag{3}$$

where

δ : rotor angle

ω : rotor speed

M : inertia constant

P_e : electrical power output of generator

P_m : mechanical power input to generator

δ_o : initial steady state rotor angle

P_e is a function of S and the control variables V, I, ϕ and ψ. P_e is given by

$$P_e = cV\cos\phi + dV\sin\phi + fI\cos\psi + gI\sin\psi + l \tag{4}$$

The real power constraint on the UPFC is given by

$$mV^2 + nI^2 + oV\cos\phi + pV\sin\phi + qI\cos\psi + rI\sin\psi + sVI\sin(\gamma - \phi) = 0 \tag{5}$$

The expressions for the coefficients c to s are given in the appendix. The following constraints are imposed on the ratings of the series and shunt converters.

$$0 < V < V_s \tag{6}$$

$$0 < I < I_s \tag{7}$$

The energy margin W_{em} given by the difference between the critical energy and the energy at the instant of fault clearing, is a quantitative measure of transient stability. The critical energy is the energy at the controlling unstable equilibrium point (UEP) $(\delta_u, 0)$.

$$W_{em} = \int_{\delta_{cl}}^{\delta_u} (P_e - P_m)\mathrm{d}\delta - \frac{1}{2} M\omega_{cl}^2 \tag{8}$$

where the subscript cl indicates quantities at the instant of fault clearing. Maximal improvement in transient stability can be achieved by maximizing the energy margin. The second term on the RHS of (8) is independent of control. The rotor angle at the controlling UEP δ_u depends on control. By applying Pontryagin's principle [11], maximization of the functional on the RHS of (8) requires maximizing the Hamiltonian H defined as

$$H = P_e - P_m \tag{9}$$

Since P_m is a constant, maximization of energy margin implies maximization of P_e w.r.t. control variables subject to the constraints (5), (6) and (7). Since P_e does not depend on any derivative of the control variables w.r.t. δ, the problem is reduced to maximizing a function for a given value of δ.

EXTENSION TO MULTIMACHINE SYSTEM

When a power system becomes unstable, it initially splits into two groups. There is usually a unique cutset consisting of series elements (connecting the two areas) across which the angle becomes unbounded. The system can be represented by two areas connected by the critical cutset as shown in fig. 2. The two areas can be assumed to be coherent in order to neglect the oscillations within the areas and account only for interarea oscillations which contribute to system separation. Locating UPFC in one of the lines belonging to the critical cutset strengthens the system and improves transient stability. By the assumption of coherent areas, the system kinetic and potential energies are given by (the derivation is given in [10])

$$W_1 = \frac{1}{2} M_{eq} \left(\frac{\mathrm{d}\delta_k}{\mathrm{d}t} \right)^2 \tag{10}$$

$$W_2 = T_k \int_{\delta_{k1}}^{\delta_k} (P_k - P_{ks})\mathrm{d}\delta_k \tag{11}$$

where M_{eq} is the equivalent inertia constant, δ_k is the angle across any line k in the critical cutset, T_k is a constant, P_k is power flow in line k, δ_{ko} is the initial value of δ_k and P_{ks} is the steady state value of P_k.

$$M_{eq} = \frac{M_I M_{II}}{M_I + M_{II}}, \quad M_I = \sum_{i \in area I} M_i, \quad M_{II} = \sum_{i \in area II} M_i$$

The energy function given by (10) and (11) is also applicable for the detailed (1.1) model of the generators; a lossless network is assumed in the derivation of the energy function.

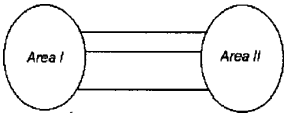

Fig. 2 Coherent areas

The energy margin is given by

$$W_{em} = T_k \int_{\delta_{kcl}}^{\delta_{ku}} (P_k - P_{ks})\mathrm{d}\delta_k - \frac{1}{2} M_{eq} \left(\frac{\mathrm{d}\delta_{kcl}}{\mathrm{d}t} \right)^2 \tag{12}$$

where δ_{ku} is the angle across the line at which $P_k = P_{ks}$. The second term on the RHS of (12) is independent of control. The angle δ_{ku} depends on control. The expression for the energy margin is similar to that for the SMIB system given by (8). The control strategy derived for the SMIB system is extended to multimachine systems and the power flow P_k on a critical line is maximized to improve transient stability.

If a UPFC is placed in one of the lines belonging to the critical cutset, maximizing energy margin is equivalent to programming the power angle relationship in the transmission line in which UPFC is situated. The system external to the line in which UPFC is situated, is represented by a Thevenin equivalent network on either side of the line. Fig. 1 is also the equivalent circuit for the multimachine case, with the only difference being that the power flow P_k considered is the power at the input port of UPFC.

The power flow P_k in the line in which UPFC is situated, is given by

$$P_k = AV^2 + BI^2 + CV\cos\phi + DV\sin\phi + FI\cos\psi + GI\sin\psi + HVI\cos(\psi - \phi) + KVI\sin(\psi - \phi) + L \quad (13)$$

The expressions for the coefficients A to L are given in the appendix. P_k is maximized subject to the constraints (5), (6) and (7).

CASE STUDIES

SMIB System

Case studies are conducted for the SMIB system to study the variation of control variables w.r.t. δ and the effect of UPFC location on the performance. The following values are assumed for the SMIB system: $E_1=E_2=1$, $R_1=R_2=0$, $X_1=X_2=0.5$, $V_{max}=0.5$, $I_{max}=0.5$, where $R_1+jX_1=Z_1\angle\theta_1$ and $R_2+jX_2=Z_2\angle\theta_2$.

If $R_1=R_2=0$, then $A=B=H=K=m=n=s=0$. For this case, it can be shown that the equations giving the necessary conditions for maximum power can be simplified to quartic equations in a single variable. Therefore the control variables for global maximum of power can be obtained. The control variables ϕ and ψ for global maximum of power are plotted in figs. 3 and 4. The voltage and current magnitudes for global maximum are the limits V_{max} and I_{max} respectively for all values of δ. The effective series impedance $R_{se}+jX_{se}$ and shunt admittance $G_{sh}+jB_{sh}$ of the UPFC are plotted in figs. 5 and 6.

The power-angle curves with and without UPFC are shown in fig. 7. The effect of location of UPFC on transient stability can be quantified by computing the area below the power-angle curve $\int_0^{\pi} P_e d\delta$ for different locations. Fig. 8 gives a plot of area below the power-angle curve w.r.t. X_1 where $X_1+X_2=1$. It can be seen that there is no significant variation in the area below the power-angle w.r.t. the location of UPFC in a line. For the values of the system parameters chosen, the optimal location of the UPFC is at the midpoint of the line. The area below the power-angle curve without UPFC is 2.

The power through the DC link (power transferred from the series branch to the shunt branch) for maximum value of power P_e is 0.125 for all values of δ. If the power through the DC link is constrained to be zero, the series and the shunt branches inject reactive voltage and reactive current respectively. The plot of the injected reactive voltage and reactive current are shown in figs. 9 and 10 respectively. The variation of current is continuous; but the voltage magnitude jumps from 0.5 to 0.191 at δ=155°. Fig. 11 shows the plot of critical energy w.r.t. the steady state power for different cases. The last case is for DC link power at zero and V and I constrained to be at their limits. It can be seen that not constraining V and I to be at their limits will be helpful at lower values of steady state power.

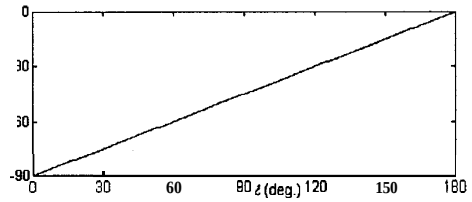

Fig. 3 Phase angle of series voltage injected by UPFC

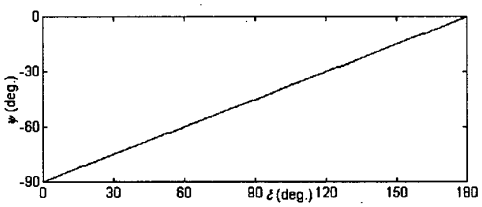

Fig. 4 Phase angle of shunt current injected by UPFC

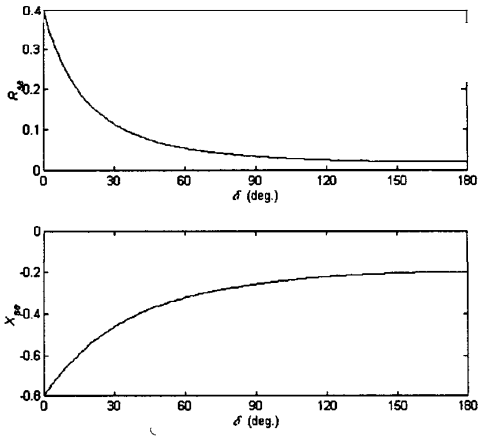

Fig. 5 Effective series resistance and reactance of UPFC

Multimachine System

The New England system (the system data are given in **[2])** is considered for the multimachine study. The generators are represented by detailed **(1.1)** model with excitation system. Loads are modelled as constant impedances. Network losses are ignored.

Fig. **12** shows the swing curves for a fault at **#14** cleared by opening the line **14-34** at **0.346 s**. The system is critically unstable; generator **2** separates from the rest of the system. It can be seen from fig. **13** that the angle across the lines **11-12** and **18-19** become unbounded. **A** UPFC is located in the line **11-12** at bus **#11**. The power flow in the line **11-12** is maximized in the post-fault period using UPFC. A rating of 0.5 pu is used for the series voltage and shunt current of the UPFC. With UPFC, the system is stable for the same fault as shown by the swing curves in fig. **14** and the critical clearing time increases from **0.345-0.346 s** to **0.356-0.357 s**. Fig. **15** gives the plot of the power transferred from the series branch to the shunt branch of the UPFC; the discontinuity in the plot is due to the discontinuities in the magnitude and angle of the shunt current injected by the UPFC. The power transfer on the line with and without UPFC are plotted in fig. **16.**

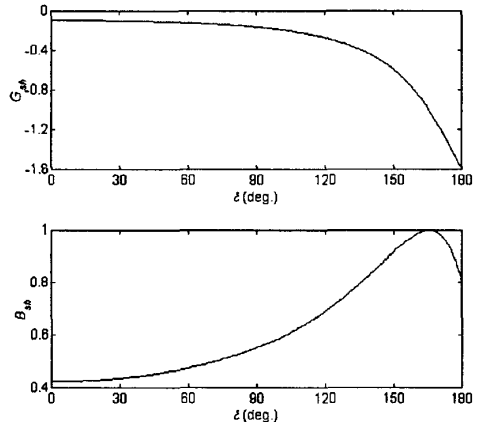

Fig. **6** Effective shunt conductance and susceptance of UPFC

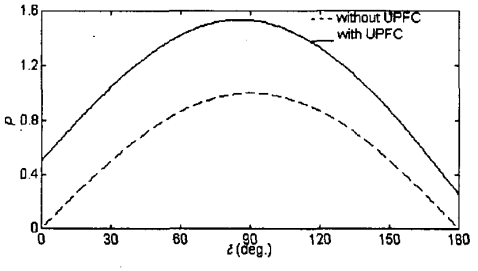

Fig. **7** Power-angle curve

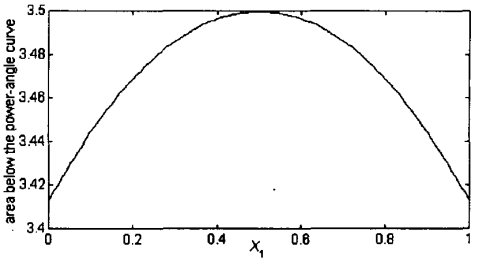

Fig. **8** Variation of area below the power-angle curve w.r.t. location of UPFC

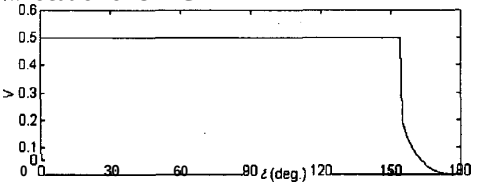

Fig. **9** Magnitude of the series voltage injected **by** UPFC (DC power=0)

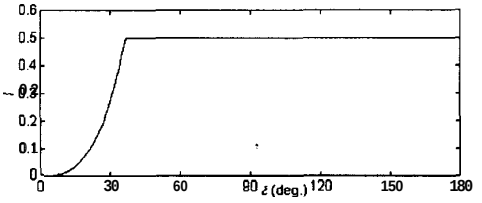

Fig. 10 Magnitude of the shunt current injected **by** UPFC (DC power=0)

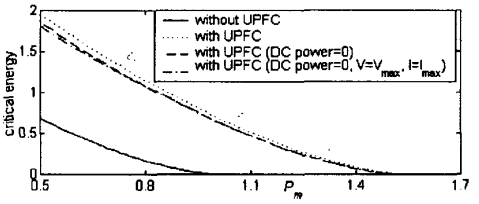

Fig. **11** Variation of critical energy w.r.t. steady state power for different cases

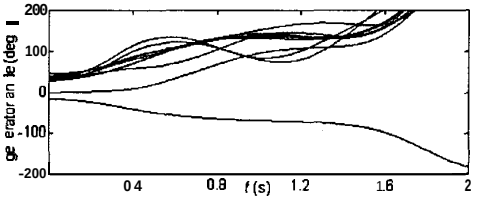

Fig. **12** Swing curves without UPFC

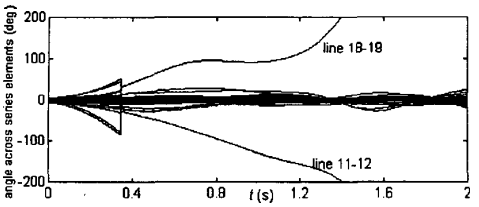

Fig. 13 Angle across series elements for unstable case

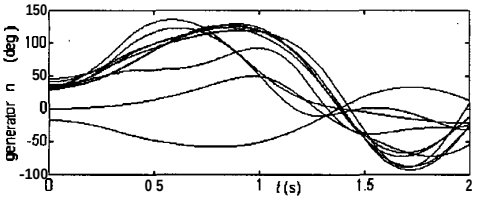

Fig. **14** Swing curves with UPFC

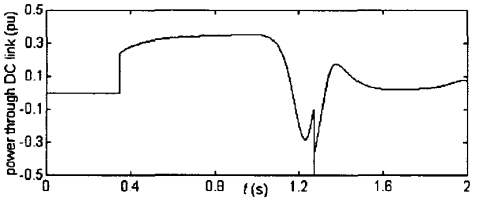

Fig. **15** Power **through** the DC link

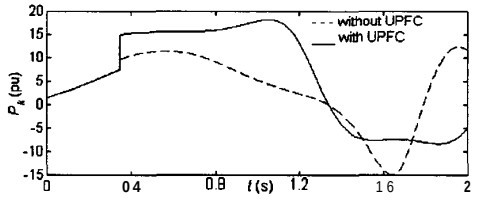

Fig. 16 Power transfer on the line

DISCUSSION

The control variables are chosen **as** the magnitude and angle of the injected series voltage and shunt current. The constraints on the ratings of the series and shunt converters can be easily expressed due to the selection of these control variables. **This** is in contrast to using the effective shunt susceptance B_{sh} **as** a control. variable for the shunt branch **in [7]**. Moreover unlike **in [7]**, B_{sh} need not be constant (at the limit) at **all** values of δ as shown in fig. 6.

When the power through the DC link is constrained to be zero, the optimal magnitudes of the injected voltage and current are not at the limits for large and **small** values of δ respectively. This illustrates that for small values of δ a **SSSC** will be helpful in increasing the power transfer, whereas for large values of δ a STATCOM will be more effective.

The control variables resulting in global maximum of power can be easily obtained for a lossless (R_1=R_2=0) circuit. For the multimachme system, though the network is lossless, R_1 and R_2 are not zero due to the real power loads. The solution obtained for the lossless circuit is used as starting values for the iterative solution for the circuit with losses.

It was found from different case studies on the New England system that for many contingencies, generator 2 separates from the rest of the system because of its large inertia constant. For **this** mode of instability, the angle across the lines 11-12 and 18-19 become unbounded. Locating UPFC in one of these lines strengthens the system and aids in improving transient stability.

CONCLUSION

A control strategy is derived for maximal improvement in transient stability by maximizing the energy **margin.** The control strategy is to maximize the power transfer from one area to the other, and is applicable to any controller which can affect the power flow in a line. The control scheme is applied to a UPFC considering the constraints on the ratings of the converters. Suitable location of the UPFC for transient stability improvement can be one of the lines across which the angle becomes unbounded in case of instability; these lines can be identified by simulation studies.

APPENDM

$$c = -\frac{E_1}{Z}\cos(\delta+\theta)$$

$$d = -\frac{E_1}{Z}\sin(\delta+\theta)$$

$$f = -\frac{E_1 Z_2}{Z}\cos(\delta-\theta_2+\theta)$$

$$g = -\frac{E_1 Z_2}{Z}\sin(\delta-\theta_2+\theta)$$

$$l = \frac{E_1^2}{Z}\cos\theta - \frac{E_1 E_2}{Z}\cos(\delta+\theta)$$

$$m = \frac{1}{Z_2}\cos\theta_2 - \frac{Z_1}{ZZ_2}\cos(\theta+\theta_2-\theta_1)$$

$$n = \frac{Z_1 Z_2}{Z}\cos(\theta_1+\theta_2-\theta)$$

$$o = -\frac{E_1}{Z_2}\cos(\theta_2-\delta) + \frac{E_1 Z_1}{ZZ_2}\cos(\theta+\theta_2-\delta-\theta_1)$$
$$-\frac{E_2 Z_1}{ZZ_2}\cos(\theta-\theta_1+\theta_2) + \frac{E_2}{Z_2}\cos\theta_2$$

$$p = \frac{E_1}{Z_2}\sin(\theta_2-\delta) - \frac{E_1Z_1}{ZZ_2}\sin(\theta+\theta_2-\delta-\theta_1) + \frac{E_2Z_1}{ZZ_2}\sin(\theta-\theta_1+\theta_2) - \frac{E_2}{Z_2}\sin\theta_2$$

$$q = E_1\cos\delta - \frac{E_1Z_1}{Z}\cos(\delta+\theta_1-\theta) + \frac{E_2Z_1}{Z}\cos(\theta_1-\theta)$$

$$r = E_1\sin\delta - \frac{E_1Z_1}{Z}\sin(\delta+\theta_1-\theta) + \frac{E_2Z_1}{Z}\sin(\theta_1-\theta)$$

$$s = \frac{2Z_1}{Z}\sin(\theta_1-\theta)$$

$$A = -\frac{Z_1}{Z^2}\cos\theta_1$$

$$B = -\frac{Z_1Z_2^2}{Z^2}\cos\theta_1$$

$$C = -\frac{E_1}{Z}\cos(\delta+\theta) + \frac{E_1Z_1}{Z^2}\cos(\delta+\theta_1) + \frac{E_2Z_1}{Z^2}\cos(\theta_1-\delta) - \frac{2E_2Z_1}{Z^2}\cos\theta_1$$

$$D = -\frac{E_1}{Z}\sin(\delta+\theta) + \frac{E_1Z_1}{Z^2}\sin(\delta+\theta_1) - \frac{E_1Z_1}{Z^2}\sin(\theta_1-\delta)$$

$$F = -\frac{E_1Z_2}{Z}\cos(\delta-\theta_2+\theta) + \frac{E_1Z_1Z_2}{Z^2}\cos(\delta+\theta_1-\theta_2) - \frac{E_2Z_1Z_2}{Z^2}\cos(\theta_1-\theta_2) + \frac{E_1Z_1Z_2}{Z^2}\cos(\theta_1+\theta_2-\delta) - \frac{E_2Z_1Z_2}{Z^2}\cos(\theta_1+\theta_2)$$

$$G = -\frac{E_1Z_2}{Z}\sin(\delta-\theta_2+\theta) + \frac{E_1Z_1Z_2}{Z^2}\sin(\delta+\theta_1-\theta_2) - \frac{E_2Z_1Z_2}{Z^2}\sin(\theta_1-\theta_2) - \frac{E_1Z_1Z_2}{Z^2}\sin(\theta_1+\theta_2-\delta) + \frac{E_2Z_1Z_2}{Z^2}\sin(\theta_1+\theta_2)$$

$$H = -\frac{Z_1Z_2}{Z^2}\cos(\theta_1-\theta_2) - \frac{Z_1Z_2}{Z^2}\cos(\theta_1+\theta_2)$$

$$K = -\frac{Z_1Z_2}{Z^2}\sin(\theta_1-\theta_2) + \frac{Z_1Z_2}{Z^2}\sin(\theta_1+\theta_2)$$

$$L = \frac{E_1^2}{Z}\cos\theta - \frac{E_1E_2}{Z}\cos(\delta+\theta) - \frac{E_1^2Z_1}{Z^2}\cos\theta_1 + \frac{E_1E_2Z_1}{Z^2}\cos(\delta+\theta_1) + \frac{E_1E_2Z_1}{Z^2}\cos(\theta_1-\delta) - \frac{E_2^2Z_1}{Z^2}\cos\theta_1$$

where $Z\angle\theta = Z_1\angle\theta_1 + Z_2\angle\theta_2$.

ACKNOWLEDGEMENT

The financial support received from the Dept. of Science and Technology, Govt. of India under the project titled "Dynamic security assessment and control of power grids" is gratefully acknowledged.

REFERENCES

1. Task Force on Discrete Supplementary Controls of the Dynamic System Performance Working Group of the IEEE Power System Engineering Committee, 1978, "A Description of Discrete Supplementary Controls for Stability", IEEE Tran. Power Apparatus and Systems, PAS-97, 149-165.

2. K.R. Padiyar, 1996, "Power System Dynamics: Stability and Control", John Wiley and Interline.

3. CIGRE Task Force 38.02.17, 2000, "Advanced Angle Stability Controls", Technical Brochure, Ref. no. 155.

4. Narain G. Hingorani and Laszlo Gyugyi, 2000, "Understanding FACTS: Concepts and Technology of Flexible AC Transmission Systems", IEEE Press, New York.

5. K.R. Padiyar and A.M. Kulkarni, 1998, "Control Design and Simulation of Unified Power Flow Controller", IEEE Tran. Power Delivery, 13, 1348-1354.

6. K.R. Padiyar and K. Uma Rao, 1999, "Modeling and Control of Unified Power Flow Controller for Transient Stability", Int. J. Electrical Power and Energy Systems, 21, 1-11.

7. R. Mihalic, P. Zunko and D. Povh, 1996, "Improvement of Transient Stability Using Unified Power Flow Controller", IEEE Tran. Power Delivery, 11, 485-492.

8. J. Bian, D.G. Ramey, R.J. Nelson and A. Edris, 1997, "A Study of Equipment Sizes and Constraints for a Unified Power Flow Controller", IEEE Tran. Power Delivery, 12, 1385-1391.

9. K.R. Padiyar and K. Uma Rao, 1997, "Discrete Control of Series Compensation for Stability Improvement in Power Systems", Int. J. Electrical Power and Energy Systems, 19, 311-319.

10. K.R. Padiyar and S. Krishna, 2001, "On-Line Detection of Loss of Synchronism Using Locally Measurable Quantities", Preprint.

11. Ian McCausland, 1969, "Introduction to Optimal Control", John Wiley & Sons.